Parameterization of the Vertical Velocity in Shallow Cumulus Clouds

Conditionally Sampled Vertical Velocity Budgets
from Large–Eddy Simulation Results

Bachelor Thesis
May 13, 2009
Yoerik de Voogd

Supervisors Dr. S.R. de Roode
Prof. Dr. A.P. Siebesma

Department of Multi Scale Physics
Faculty of Applied Sciences

Delft University of Technology

Abstract

Shallow cumulus clouds play an important role in the energy transport through the atmosphere. For general circulation models (such as weather prediction models) these clouds are important. Due to the relative small size of these clouds compared to the typical grid-size used by these models, the vertical transport by cumuli is a subgrid phenomenon which needs parameterization. In this research the parameterized cloud–core vertical velocity equation is studied in more detail. To this end we have examined the vertical velocity within shallow cumulus clouds using Large Eddy Simulation models (LES) to test and possibly improve the parameterization. Besides, we also try to gain a better understanding of the physical meaning of this approximation.

We found that describing the vertical velocity using only the buoyancy and lateral mixing, as is already done, can give accurate results. In this method pressure and subplume effects are incorporated by scaling the buoyancy and lateral mixing. The two cases studied, BOMEX and ARM, both showed that subplume effects are very small and can be neglected, whilst pressure effects can be complete incorporated by damping the buoyancy. Unfortunately the amount of damping required to accurately describe the vertical velocity in this way is not constant between the cases.

Examination of the fractional entrainment computed from the conditionally sampled vertical velocity equation and from the total specific humidity showed a distinct difference for the ARM case. This difference can possibly be the effect of the subsiding shell around the clouds. This shell around the clouds can have both a positive or a negative vertical velocity, thus either move up or down. It seems plausible that for BOMEX the vertical velocity of this shell is downward (negative), whilst it is upward (positive) for the ARM case. This difference has an impact on the fractional entrainment and therefore possibly on the relative damping of the buoyancy caused by the pressure.

Contents

1 Introduction

Clouds exist in many different sizes and shapes. Some rain, some thunder and all just block the sunlight. Clouds are usually categorised based on the height at which they form. The atmosphere is roughly divided into three layers. The lowest of the three is the so called atmospheric boundary layer (ABL). This is the part of the atmosphere influenced by the earth's surface.

Within the atmospheric boundary layer again the clouds can be categorised. This is done in two groups. Clouds that cover (almost) the entire sky and clouds that cover 5–20 % of the sky. The latter are known as shallow cumulus clouds. Usually these clouds are associated with good weather and are therefore sometimes referred to as fair–weather clouds.

These clouds play an important role in the energy transported through the air. Therefore they are important aspects of weather and climate forecasting. These forecasts are usually performed using general circulation models (GCMs) These models cannot directly calculate the effects of shallow cumulus clouds because the typical size of such a cloud (< 1 km) is much smaller than the typical grid size of these models ($\sim$ 10–100 km). Therefore parametrizations are needed.

In order to find these parametrizations the clouds have to be studied in more detail. Ideally this should be done using measurements with airplanes. However, this is very difficult and costly to do, because data is required over a long period of time at many different heights in the cloud layer. An alternative are Large Eddy Simulations (LES). Multiple studies (Neggers et al., 2003; Siebesma et al., 2003) have compared LES models with the few atmospheric measurements that are performed and concluded that LES models are capable of accurately computing the dynamics of shallow cumulus clouds.

In this research the parametrization of shallow cumulus convection for GCMs is analysed using a LES model. In particular we focus on the vertical velocity of the clouds. The aim is to verify whether the current parametrization is capable of correctly predicting this vertical velocity and to compare the various forces influencing the vertical velocity within the shallow cumulus clouds with the contributions that are used in the parametrization. The vertical velocity of the clouds is important to know in GCMs because the fractional entrainment of the clouds is currently thought to be proportional to the inverse of the vertical velocity (Gregory, 2001). To correctly use this fractional entrainment a better calculation method is required for the vertical velocity in GCMs.

For this research we use the initial profiles as measured during the Barbados Oceanographic and Meteorological Experiment (BOMEX) (Holland and Rasmusson, 1973) and the Atmospheric Radiation Measurement Program (ARM) (Brown et al., 2002). The BOMEX case is commonly used for LES models because the measurements can be used to test the model and during large parts of the experiment relatively stable shallow cumulus clouds developed. The ARM case is, contrary to the BOMEX case, over land. The ARM case is chosen because the surface fluxes are very different and exhibit a clear diurnal cycle, making it a good case to compare to the BOMEX case.

2 Theory

This chapter gives a theoretical overview of clouds. First the basis of cloud formation will be discussed, followed by some definitions of variables commonly used in meteorological research. After this there will be an explanation of the LES model and its governing equations followed by an outline of the sampling procedures used on the LES data. Finally some definitions, used in the remainder of the report, will be discussed.

2.1 Cloud formation

Cloud formation in the atmospheric boundary layer is indirectly dominated by the sun. The sun heats the earth's surface which, in turn, heats the air parcels above the surface. These parcels of air rise in thermals through the subcloud layer. If the air parcel is dry, it cannot overcome the relatively more buoyant layer that tops the subcloud layer. However, if the parcel contains sufficient moisture the parcel can become saturated. Above the height at which this happens, which defines the Lifting Condensation Level (LCL), water vapour starts condensating. The heat released during this condensation increases the buoyancy of the parcel, as can be seen in the slope of the dotted line in figure (2.1). If buoyancy increase and the vertical velocity of the cloud with respect to its environment are not high enough to reach the Level of Free Convection (LFC), the level where the buoyancy becomes positive, the developing cloud is limited between the LCL and the LFC. This is called a forced cloud.

If the latent heat release is large enough to reach positive buoyancy, the cloud will reach the LFC. Here the virtual temperature of the environment is smaller then that of the cloud parcel. Now the parcel has turned into an active cloud parcel and due to condensation will gain buoyancy and accelerate upwards. This process will eventually end, either because the parcel reaches the inversion layer, where the temperature of the environment is much larger than that of the cloud or because mixing with the drier environment in the cloud top lowers the water content below the saturation level. Some parcels can have sufficient upward vertical velocity to move well within the inversion layer where they will become separated from the bulk of the cloud (becoming passive clouds) and eventually mix with the environment and disappear. This all is illustrated in figure 2.1 originally by Heus (2008).

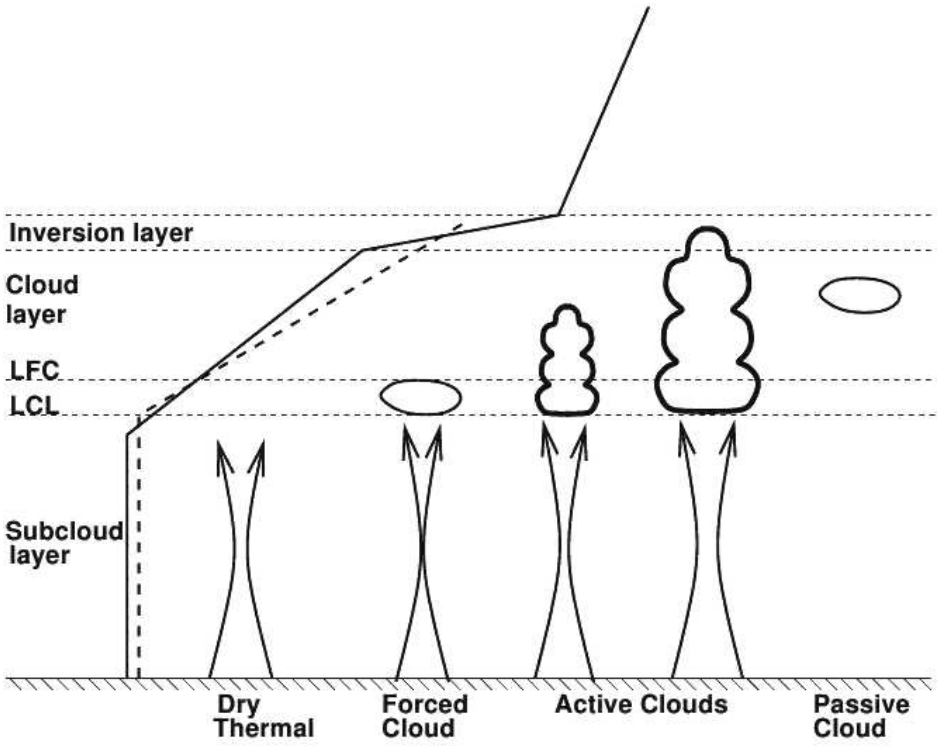

Figure 2.1: A schematic overview of an atmospheric boundary layer containing cumulus clouds. The full line depicts the virtual potential temperature of the environment; the dashed line is the virtual potential temperature of an (active) cloud and the thermal beneath the cloud, from Heus (2008).

An air parcel is, obviously, not an isolated cubic entity. It will interact with its surrounding environment and thus, there will be exchange of energy, momentum and moisture with the environment both on the sides of the cloud (lateral) and on the top. This mixing tends to reduce the vertical velocity of the parcel since the vertical velocity of parcels outside the cloud is lower.

2.2 Basic variables in meteorological research

The velocity of particles can, in theory, be calculated using the so called Navier-Stokes equation. Before arriving at the Navier-Stokes equation some basic variables, common in meteorological research, have to be specified. In meteorological research a few different variables are used to describe the state of the atmosphere. The first one is the specific humidity (q_k). This dimensionless variable tells something about the amount of water in the parcel of air.

$$q_k = \frac{m_k}{m} \qquad \text{where } k \in v, l, i \tag{2.1}$$

Here v, l, i are respectively vapour, liquid and ice, m is the total mass: $m = m_v + m_l + m_i + m_d$ where m_d is the mass of dry air.

Now we also want to add the effect of water vapour and liquid water on the density. The total mass of a parcel of air is now given by $m = m_v + m_l + m_d$, where we do not consider water in the ice phase, because ice does not form in shallow cumulus clouds. The total volume is now given by $V = V_g + V_l$, where the subscript g denotes the volume occupied by the gasses. This gives for the density of the mixture:

$$\rho = \frac{m_d + m_v + m_l}{V} \tag{2.2}$$

By comparing this with the density of dry air and using (2.1) this results in:

$$\frac{\rho_d}{\rho} = 1 - q_v - q_l \tag{2.3}$$

Applying the ideal gas law and rearranging it a bit finally gives:

$$p = \rho R_m T = \rho \left[(1 - q_v - q_l) R_d + q_v R_v \right] T = \rho R_d T_v \tag{2.4}$$

Where R_m is the gas constant of the mixture, R_d the gas constant of dry air, R_v gas constant of water vapour and T_v the virtual temperature defined as:

$$T_v = \left[1 - \left(1 - \frac{1}{\varepsilon} \right) q_v - q_l \right] T \tag{2.5}$$

Where $\varepsilon = \frac{R_d}{R_v} \approx 0.622$ (de Roode, 2004).

Using the second law of thermodynamics:

$$Tds = du + pdv \geq 0 \tag{2.6}$$

Here s is the entropy, u the internal energy, v the volume and p the pressure.

A potential temperature θ is now defined as:

$$ds = c_p dln\theta \tag{2.7}$$

Here c_p is the specific heat capacity under constant pressure. Combining all of this gives:

$$s - s_0 \quad = \quad c_p \left(ln\theta - ln\theta_0\right) = c_p ln \left[\frac{T}{T_0}\left(\frac{p_0}{p}\right)^{\frac{R_d}{c_p}}\right] \tag{2.8}$$

For a isentropic process ($ds = 0$) and by setting $T_0 = \theta$ this gives a potential temperature:

$$\theta = T\left(\frac{p_0}{p}\right)^{\frac{R_d}{c_p}} \tag{2.9}$$

Now combining this potential temperature with the virtual temperature defined in equation (2.5) we can define a virtual potential temperature:

$$\theta_v = T_v\left(\frac{p_0}{p}\right)^{\frac{R_d}{c_p}} \tag{2.10}$$

The virtual potential temperature can be seen as the virtual temperature a parcel of air would obtain if it would be expanded or compressed adiabatically to a standard pressure of 1000 hPa. Therefore it is conserved during dry adiabatic processes ($d\theta = 0$ and $dq_l = 0$).

If we want to incorporate phase changes we can define a potential liquid water temperature as:

$$\theta_l = \theta e^{-\frac{L_v q_l}{c_p T}} \approx \theta - \frac{L_v}{c_p \Pi} q_l \tag{2.11}$$

Where $\Pi = \left(\frac{p}{p_0}\right)^{\frac{R_d}{c_p}}$ is the Exner function. This variable will be conserved as long as there is no precipitation that removes liquid water and no evaporation of raindrops in unsaturated air.

The buoyancy B can be described by the above derived variables:

$$B = \frac{g}{\theta_0}\left(\theta_v - \overline{\theta_v}\right) \tag{2.12}$$

Here the overbar denotes the slab averaged value and θ_0 is the reference state potential temperature.

2.3 LES model

Now that we know the basic instruments of meteorological research we can have a look at the LES model used. The atmospheric boundary layer, where shallow cumulus clouds develop, is dominated by turbulent eddies whose typical dominant length scales are of the order of $\sim$ 1 km. These turbulent motions can be calculated using the Navier-Stokes equations for incompressible flow in a rotating reference system. Density variations can be ignored except in the buoyancy term, so we are within the Boussinesq approximation (Cuijpers, 1994).

In theory these equations can be solved, but to solve them from the smallest (Kolmogorov ($\sim$ 1mm)) to the largest length scale ($\sim$ 1km) would require approximately 10^{18} gridpoints. Far more than any current state of the art computer can calculate. However, since the flow in the atmospheric boundary layer is primarily dominated by the large eddies, it can be simulated using Large-Eddy simulation models. In these models the large eddies are calculated explicitly, while the effects of small scale motions, scales smaller than the gridbox size, on the turbulent transport are parameterized.

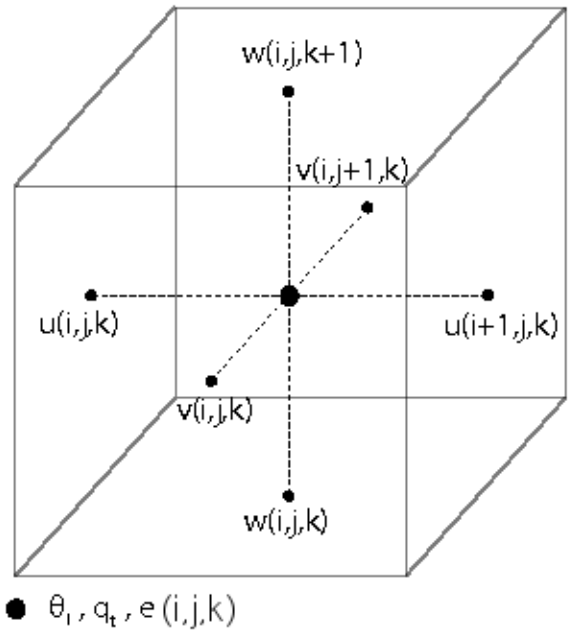

Figure 2.2: Grid box of the LES model with the positions of the variables that describe the governing equations.

The variables resolved by the model are u, v and w, the three directions (x,y,z) of the velocity vector and θ_l and q_t, because they are conserved for moist adiabatic processes (van Zanten, 2000). Also solved is the subgrid turbulent kinetic energy (e). The various variables are calculated at different positions of a grid box, as shown in figure 2.2.

2.4 Governing Equations

The equations that govern the flow in the LES model are the conservation equations of momentum (Navier-Stokes), conservation equation of mass (continuity equation) and the conservation equations of liquid water potential temperature (θ_l) and total water specific humidity (q_t) (van Zanten, 2000),

$$\frac{\partial \psi}{\partial t} = -\frac{\partial u_j \psi}{\partial x_j} - \frac{\partial \overline{u_j'' \psi''}}{\partial x_j} + S_\psi \tag{2.13}$$

Here the variable ψ represents either q_t or θ_l. $\overline{u_j'' \psi''}$ denotes subgrid flux terms. The source term S_ψ represents processes like radiation and precipitation.

The Navier-Stokes equations for the LES model read:

$$\frac{\partial u_i}{\partial t} = \frac{g}{\theta_0}\left(\theta_v - \overline{\theta_v}\right)\delta_{i3} - \frac{\partial u_i u_j}{\partial x_j} - \frac{\partial \pi}{\partial x_i} - \frac{\partial \tau_{ij}}{\partial x_j} \tag{2.14}$$

Here u_i represents either u, v or w the velocity components in $x_i = (x, y, z)$ directions. Use has been made of the modified pressure π (Deardoff, 1973). t is the time and g the gravitational acceleration. The first term on the right hand side is the buoyancy as described in equation (2.12); δ_{ij} is the Kronecker delta and τ_{ij} is a subgrid flux term. The subgrid terms in equations (2.13) and (2.14) use the following parameterization:

$$\overline{u_j'' \psi''} = -K_\psi \frac{\partial \psi}{\partial x_j} \tag{2.15}$$

$$\tau_{ij} = -K_m \left(\frac{\partial u_i}{\partial x_j} + \frac{\partial u_j}{\partial x_i}\right) \tag{2.16}$$

Here K_m is the eddy viscosity and K_ψ the eddy diffusity (de Roode and Bretherton, 2003). These two parameters are evaluated using the prognostic equation for the subgrid kinetic turbulent energy (e), which reads:

$$\frac{\partial e}{\partial t} = -u_j \frac{\partial e}{\partial x_j} - \tau_{ij}\frac{\partial u_i}{\partial x_j} + \frac{g}{\theta_0}\overline{w''\theta_v''} - \frac{\partial \overline{w'' e''}}{\partial x_j} - \frac{1}{\rho_0}\frac{\partial \overline{w'' p''}}{\partial x_j} - \varepsilon \tag{2.17}$$

Here ε is the dissipation rate. The exact representation and the formulation used to actually calculate all terms are very accurately described by Heus (2008).

Finally the conservation equation of mass (continuity equation) for the LES model is the continuity equation for an incompressible flow (constant density):

$$\frac{\partial u}{\partial x} + \frac{\partial v}{\partial y} + \frac{\partial w}{\partial z} = 0 \tag{2.18}$$

Every model requires, besides the governing equations, initialisation to be specified. These inputs include the starting vertical profiles of the temperature, humidity and the two horizontal wind velocity components. Also descriptions of the large scale forcings, processes acting on a larger scale than the domain of the LES have to be specified. As a result of the use of initial profiles the first few hours of simulation are usually considered useless due to the gradual increase of resolved turbulence that generates the horizontal variations in temperature and humidity, this is known as the spin-up phase. The initial profiles for the BOMEX case are derived from the BOMEX measurements as described in detail by Holland and Rasmusson (1973). While the initial profiles for the ARM case are derived from the ARM measurements as described in detail by Brown et al. (2002).

2.5 Sampling procedures

For the numerical analysis only the cloud core data is selected. The cloud core is defined as that part of the cloud where the virtual potential temperature is higher than the slab average virtual potential temperature, liquid water is present and there exists a vertical flow upwards, so:

$$\begin{aligned} w &> 0 \\ \theta_v &> \overline{\theta_v} \\ q_l &> 0 \end{aligned} \tag{2.19}$$

This means that all the calculated variables must be sampled. For the sampling an all or nothing approach is used. So a gridpoint either satisfies the conditions or not. The conditionally sampled horizontal slab–mean values $[\psi]_s$ are then calculated using (de Roode and Bretherton, 2003):

$$[\psi]_s = \frac{\int_A I_s \, \psi \, dA}{\int_A I_s \, dA} \tag{2.20}$$

The integration is over a slab at height z and I_s is one if the conditions are met, else it is zero. The fraction (σ_s) of gridpoints that satisfy the conditions is then given by:

$$\sigma_s = \frac{\int_A I_s \, dA}{\int_A dA} \tag{2.21}$$

The integrals are evaluated by summation over discrete gridpoints in the LES model.

2.6 Definitions

For notational convenience the square brackets denoting the sampling will be omitted when concerning the vertical velocity so:

$$[w]_s = w_s \tag{2.22}$$

Another important part of this research uses the massflux. This is defined as:

$$M_s = \rho\sigma_s \left(w_s - \overline{w}\right) \tag{2.23}$$

Since the density is often separated from the equations it is common to use a slightly modified form. Also the slab averaged vertical velocity is typically very small and thus neglected:

$$M_s' = \sigma_s w_s \tag{2.24}$$

For notational simplicity the prime will be omitted from now on. The change of the massflux with height is governed by the conditionally sampled conservation of mass equation:

$$\frac{\partial M_s}{\partial z} = -\frac{\partial \sigma_s}{\partial t} + E_w - D_w \tag{2.25}$$

Here E_w and D_w are respectively the lateral entrainment and detrainment for vertical momentum.

3 Parameterization

3.1 Current Method

With all the mathematics and principles explained it is time to look at the parameterization. It all originates from an article written by Simpson and Wiggert (1969).

The whole idea of the parameterization is based on the fact that it should be possible to model the behaviour of an ensemble of clouds as one big cloud. The basis comes from a model of a spherical bubble rising in a coordinate system relative to the earth done by Levine (1959) where he derives an equation for the vertical velocity of the centre of mass of a bubble:

$$\frac{dw}{dt} = B - \frac{3}{8}\left(\frac{3}{4}K_2 + C_D\right)\frac{w^2}{R} \tag{3.1}$$

Where B is the buoyancy as defined before (2.12), K_2 a mixing parameter, C_D a drag coefficient and R the radius of the bubble. The mixing parameter and the drag coefficient where determined using lab experiments.

This idea was used for not just a bubble but for a whole cloud. Here R represents the radius of a plume cap. The model used here is that of a rising plume. Here it states, as described by Simpson et al. (1965), that the velocity with which the centre of mass of the plume cap rises is fuelled by the buoyancy while being reduced by a drag term proportional to w^2/R. By taking a coordinate system with its origin at the centre of the plume cap, which rises at a rate: $w \equiv \partial z/\partial t$ (Simpson et al., 1965) the time derivative changes to:

$$\frac{dw}{dt} = w\frac{\partial w}{\partial z} = \frac{\partial}{\partial z}\left(\frac{w^2}{2}\right) \tag{3.2}$$

With this we arrive at the form as used by Simpson and Wiggert (1969):

$$\frac{1}{2}\frac{\partial w^2}{\partial z} = B - \frac{3}{8}\left(\frac{3}{4}K_2 + C_D\right)\frac{w^2}{R} \tag{3.3}$$

Simpson and Wiggert (1969) note that due to the deployment of equation (3.2) a steady-state is assumed.

Using lab experiments and comparison between model data and measurements Simpson and Wiggert (1969) made a few changes to equation (3.3). They noted that the drag term, introduced because the vertical momentum was reduced by a larger factor than the entrainment could account for, could better be described by reducing the buoyancy term with a virtual mass term. This introduced another constant into the equation instead of C_D. Also they used the following entrainment relation:

$$\frac{1}{M}\frac{\partial M}{\partial z} = \frac{9}{32}\frac{K_2}{R} = \varepsilon \tag{3.4}$$

Note here that this is different from the current idea that the massflux is equal to the entrainment minus the detrainment (2.25). At the time of Simpson and Wiggert (1969) detrainment was not considered and the vertical change in massflux was simply proportional to the entrainment.

Using above formula to add the fractional entrainment gives the final form as used for example by Siebesma et al. (2003):

$$\frac{1}{2}\frac{\partial {w_s}^2}{\partial z} = -b\varepsilon {w_s}^2 + aB \tag{3.5}$$

Here a and b are constants and the s subscripts have been added to denote the sampled values, corresponding with the notation used so far. It should be noted that the constant b was not added by Simpson and Wiggert (1969) but is added later. Table (3.1) gives an overview of values for the constants a and b suggested by different authors.

Table 3.1: Current values suggested for the parameterization from different authors.

Author	a	b
Simpson and Wiggert (1969)	$^2/_3$	1
Simpson[x]	$^2/_3$	2
Gregory (2001)	$^1/_3$	3
Gregory[*]	$^1/_3$	2

[*] as used in Siebesma et al. (2003), from now on referred to as Gregory 2.

[x] as used in Siebesma et al. (2003) and Gregory (2001), from now on referred to as Simpson 2.

For the constants Simpson and Wiggert (1969) thus suggested:

$$a = \frac{2}{3} \qquad \text{and} \qquad b = 1 \tag{3.6}$$

As mentioned above the constant a is based on a virtual mass coefficient and using lab experiments was found by Simpson and Wiggert (1969) to amount to the factor $a = \frac{2}{3}$. Gregory (2001) used $a = 2/3$ and $b = 2$, which differs with a factor 2 compared to Simpson and Wiggert (1969). This can possibly be attributed to using both the drag coefficient and the virtual mass, instead of only the virtual mass as suggested by Simpson and Wiggert (1969). The values found by Gregory (2001) are also the ones used by Siebesma et al. (2003).

Gregory (2001) then used a somewhat different model, because he has a different suggestion for the fractional entrainment than the way it is suggested by Simpson and Wiggert (1969). He therefore also uses a different approach for the sampled slab averaged vertical velocity:

$$\frac{1}{2}\frac{\partial w_s^2}{\partial z} = \frac{1}{6}B - \frac{1}{2}\delta w_s^2 - \varepsilon w_s^2 \tag{3.7}$$

We can rewrite this using the massflux (2.25) if we assume that the cloud cover is constant in time:

$$\frac{1}{\sigma_s w_s}\frac{\partial \sigma_s w_s}{\partial z} = \varepsilon - \delta \tag{3.8}$$

$$\frac{1}{w_s}\frac{\partial w_s}{\partial z} + \frac{1}{\sigma_s}\frac{\partial \sigma_s}{\partial z} = \varepsilon - \delta \tag{3.9}$$

Now we also have to assume that the cloud cover is constant with height, which allows us to eliminate the fractional detrainment from equation (3.7):

$$\begin{aligned}
\delta &= \varepsilon - \frac{1}{w_s}\frac{\partial w_s}{\partial z} \\
\frac{1}{2}\frac{\partial w_s^2}{\partial z} &= \frac{1}{6}B - \frac{1}{2}\left(\varepsilon - \frac{1}{w_s}\frac{\partial w_s}{\partial z}\right) w_s^2 - \varepsilon w_s^2 \\
&= \frac{1}{6}B + \frac{1}{4}\frac{\partial w_s^2}{\partial z} - \frac{3}{2}\varepsilon w_s^2 \\
&= \frac{1}{3}B - 3\varepsilon w_s^2
\end{aligned} \tag{3.10}$$

In the third step use has been made of the chain rule to bring the w_s inside the derivative. Then rearranging and ultimately multiplying by 2 gives a result comparable with the parameterization (3.5). So Gregory (2001) uses the following values for the constants:

$$a = \frac{1}{3} \qquad \text{and} \qquad b = 3 \tag{3.11}$$

This is different than those found by Siebesma et al. (2003) when analysing the article by Gregory (2001), he finds a value of $b = 2$. The difference might be caused by the fact that we have now assumed that the cloud cover is constant with height, which might be a poor approximation.

There are three different physical interpretations for the parameterization given by multiple authors. The first interpretation is given by Simpson and Wiggert (1969). They say that the pressure induces a virtual additional mass that the buoyancy transports upwards, thus downscaling the buoyancy.

The second interpretation comes from both Gregory (2001) and Neggers et al. (2003). They state that scaling of the mixing term (b) can be interpreted as integrating the effect of pressure perturbations, while the reduced buoyancy (a) is due to the loss of potential energy to sub-plume turbulence.

The last interpretation comes from Siebesma et al. (2007). He also has the same parameterization equation (3.5), but he expresses the effects of the pressure in terms of the vertical velocity variance as:

$$\frac{\partial p}{\partial z} \approx \frac{\partial \mu {w_s}^2}{\partial z} \tag{3.12}$$

Where μ is a constant taken to be $\mu = 0.15$. Using this he arrives at:

$$\frac{1}{2}(1-2\mu)\frac{\partial {w_s}^2}{\partial z} = -b\varepsilon {w_s}^2 + B \tag{3.13}$$

This is the same result as equation (3.5) but the pressure term is incorporated into the vertical velocity variance instead of the buoyancy. The different values found by the various authors are summarised above in table 3.1.

3.2 Conditionally sampled LES vertical velocity equation

To better understand the budgets that are absorbed in the constants, the equations governing the LES model (2.13, 2.14) have to be rewritten into something similar to the parameterization. First using a mass-flux approach, as made by Siebesma and Cuijpers (1995), the conditionally sampled vertical velocity can be expressed as (de Roode and Bretherton, 2003):

$$\frac{\partial \sigma_s w_s}{\partial t} = -\frac{\partial M_s w_s}{\partial z} - \frac{\partial \sigma_s \left[w'' w''\right]_s}{\partial z} + E_w w_e - D_w w_s + \sigma_s \frac{g}{\theta_0}\left(\theta_{v,s} - \overline{\theta_v}\right) - \sigma_s \left[\frac{\partial \pi}{\partial z}\right]_s \tag{3.14}$$

Here E_w and D_w are respectively the lateral entrainment and detrainment for vertical momentum, w'' the deviations from the average in–cloud vertical velocity and M_s is the mass flux. Comparing this with the original equation (2.14) directly shows the relation for the lateral entrainment and detrainment and the effect of moving the square outside the sampling operator:

$$E_w w_e - D_w w_s = -\sigma_s \left[\frac{\partial \tau_{ij}}{\partial x_j}\right]_s - \sigma_s \left[\frac{\partial uw}{\partial x}\right]_s - \sigma_s \left[\frac{\partial vw}{\partial y}\right]_s \tag{3.15}$$

$$\left[w^2\right]_s = w_s^2 + \left[w'' w''\right] \tag{3.16}$$

Here the assumption is made that all effects along the boundary can be modelled as an incoming and an outgoing term both proportional to the field, the entrainment and detrainment (Siebesma, 1998). Using this, the continuity equation for the mass flux (2.25) and the chain rule of differentiation we can rewrite equation (3.14):

$$\begin{aligned}\sigma_s \frac{\partial w_s}{\partial t} + w_s \frac{\partial \sigma_s}{\partial t} = &-\sigma_s \frac{\partial w_s^2}{\partial z} - w_s^2 \frac{\partial \sigma_s}{\partial z} - \frac{\partial \sigma_s \left[w'' w''\right]_s}{\partial z} - E_w \left(w_s - w_e\right) \\ &+ w_s \frac{\partial M_s}{\partial z} + w_s \frac{\partial \sigma_s}{\partial t} + \sigma \frac{g}{\theta_0}\left(\theta_{v,s} - \overline{\theta_v}\right) - \sigma_s \left[\frac{\partial \pi}{\partial z}\right]_s\end{aligned} \tag{3.17}$$

Applying the chain rule would normally also require the use of Leibniz' rule (Young, 1988) and would thus give rise to a boundary term. Due to the application of the mass flux approach, using an entrainment and detrainment, all terms along the boundary are already absorbed within the entrainment and detrainment. Now again using the chain rule:

$$w_s \frac{\partial M_s}{\partial z} = w_s^2 \frac{\partial \sigma_s}{\partial z} + \frac{\sigma_s}{2} \frac{\partial w_s^2}{\partial z} \tag{3.18}$$

We approximate the entrainment as follows:

$$E_w \left(w_s - w_e\right) = \varepsilon_w \sigma_s w_s \left(w_s - w_e\right) \approx \varepsilon_w \sigma_s w_s^2 \tag{3.19}$$

where use has been made of the fact that the vertical velocity of the environment is much smaller than that of the cloud.

Combining it all gives:

$$\frac{\partial w_s}{\partial t} = -\frac{1}{2}\frac{\partial w_s^2}{\partial z} - \frac{1}{\sigma_s}\frac{\partial \sigma_s \left[w''w''\right]_s}{\partial z} - \varepsilon w_s^2 + \frac{g}{\theta_0}\left(\theta_{v,s} - \overline{\theta_v}\right) - \left[\frac{\partial \pi}{\partial z}\right]_s \tag{3.20}$$

A similar approach as done above has been done by Gregory (2001). The additional density term he has, was omitted here because we are within the Boussinesq approach. With this last step equation (3.20) has a similar form as the parameterization (3.5):

$$\frac{1}{2}\frac{\partial w_s^2}{\partial z} = \frac{g}{\theta_0}\left(\theta_{v,s} - \overline{\theta_v}\right) - \varepsilon_w w_s^2 - \frac{\partial w_s}{\partial t} - \frac{1}{\sigma_s}\frac{\partial \sigma_s \left[w''w''\right]_s}{\partial z} - \left[\frac{\partial \pi}{\partial z}\right]_s \tag{3.21}$$

From this it is clear that the last three terms on the right-hand side are incorporated into the constant (a), in the case of Simpson and Wiggert (1969), or the constants (a and b), in the case of Siebesma et al. (2003) and Gregory (2001), of the parameterization (3.5).

What is left is one unknown, being the fractional entrainment ε_w. The fractional entrainment is often diagnosed using the continuity equation for a scalar:

$$\frac{\partial \sigma \psi_s}{\partial t} = -\frac{\partial M_s \psi_s}{\partial t} + E\psi_e - D\psi_s \tag{3.22}$$

When assuming a steady–state solution this becomes (Neggers et al., 2003):

$$\varepsilon_\psi = -\left(\psi_s - \overline{\psi}\right)^{-1}\frac{\partial \psi_s}{\partial z} \tag{3.23}$$

Here ψ can either be the total specific humidity q_t or the liquid–water potential temperature θ_l. When applying the parameterization one commonly assumes:

$$\varepsilon_w = \varepsilon_{q_t} \tag{3.24}$$

Unless otherwise stated all results presented are based on this assumption.

4 Results

For both cases the various budget terms as described by formula (3.21) are calculated using the LES model, while the entrainment will be calculated using the q_t budget (3.23) In the following section these budgets will be analysed for both the BOMEX and ARM case. For both cases different possibilities for the constants of the parameterization will be discussed resulting in a suggestion for these parameters for the two cases. All figures containing different budgets or other variables of the cloud core are plotted on a axis which contains the height levels where there exists a cloud core. At cloud base and even more so at the top the budgets terms can show strange behaviour, like extraordinary high or low values. For these areas the cloud core cover is so low that the numeric sampling can no longer be used to accurately describe the situation.

4.1 BOMEX case

In figure 4.1 the budget terms in the cloud layer are displayed for the 8^{th} hour of simulation, these results are fairly representative for the 3^{rd} till the 8^{th} hour. The first two hours are omitted because the system is then still in the startup phase. From this data it is clear that the buoyancy is the forcing term of the equation. However, the lateral mixing term (entrainment term) and the pressure term are both negative and of roughly equal size. This suggests a possibility for parameterization of the pressure term using the lateral mixing term. From these observations scaling the lateral mixing to account for the pressure term seems possible, at least for the lower part of the cloud.

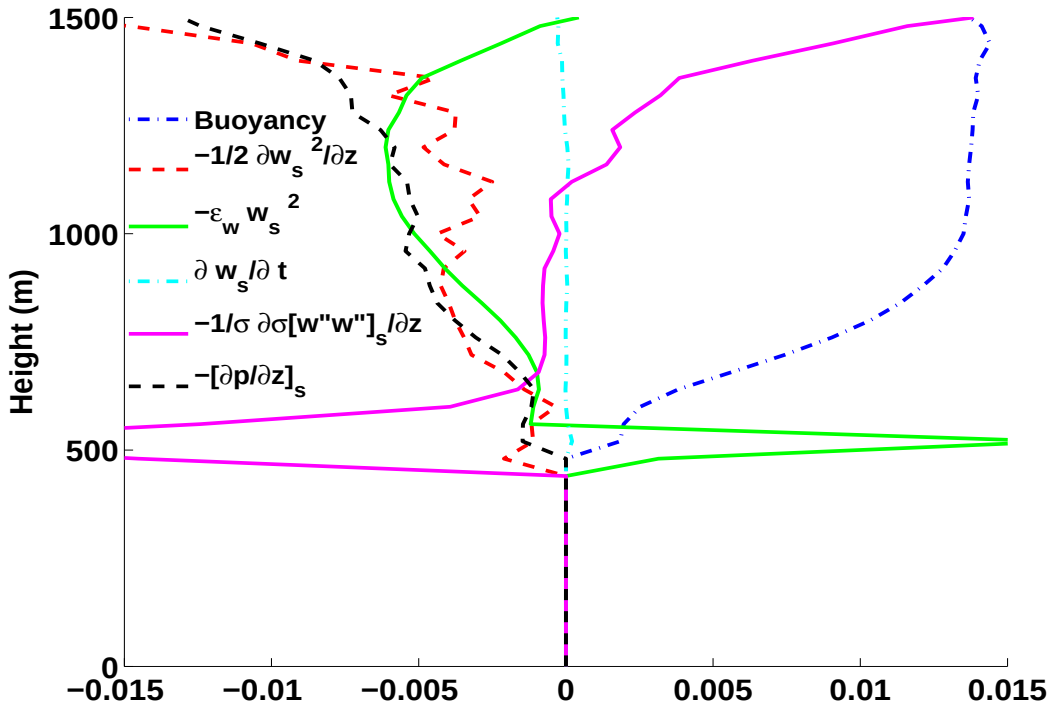

Figure 4.1: Budgets of the vertical velocity equation (3.21) for the 8^{th} hour of simulation for the BOMEX case.

The subplume term however does not seem to have any parallel with any of the other terms. It is, for instance, the only term that changes sign halfway the cloud core layer. It is also clear that the time dependence is negligible small. Unfortunately this means that there is no clear connection between the subplume term and either the buoyancy or gradient of the vertical velocity squared. Based on this data there seems to be no apparent reason to approximate the subplume term by scaling another term. However, the subplume term is not very large. It gives only a small contribution and it might be possible to neglect it.

So far there seems to be a connection between the pressure and the entrainment term. From the graph in figure 4.1 this even seems to directly suggest a value for the constant $b = 2$. This is also what currently is used in various GCMs (table 3.1). Neglecting the subplume term would give for the other constant simply $a = 1$.

We want to check the hypothesis and also compare the results found with the values suggested by other authors (table 3.1). Table (4.1) gives an overview of the various values for the constants (a and b) as suggested by different authors and the values based on the LES budgets found during this research.

Table 4.1: Suggested values for the constants of the parameterization based on literature and the BOMEX and ARM case results

Name	a	b
Simpson	$2/3$	1
Simpson 2	$2/3$	2
Gregory	$1/3$	3
Gregory 2	$1/3$	2
Result LES BOMEX	1	2
Result LES ARM	$1/3$	1

The values linked to authors are the same as found in table (3.1).

To check the hypothesis we calculate $\frac{1}{2}\frac{\partial w_s^2}{\partial z}$ using the different constants a and b, as shown in table (4.1) using the buoyancy, fractional entrainment (ε_{q_t}) and vertical velocity as calculated by the LES model and compare this with the results from the LES model.

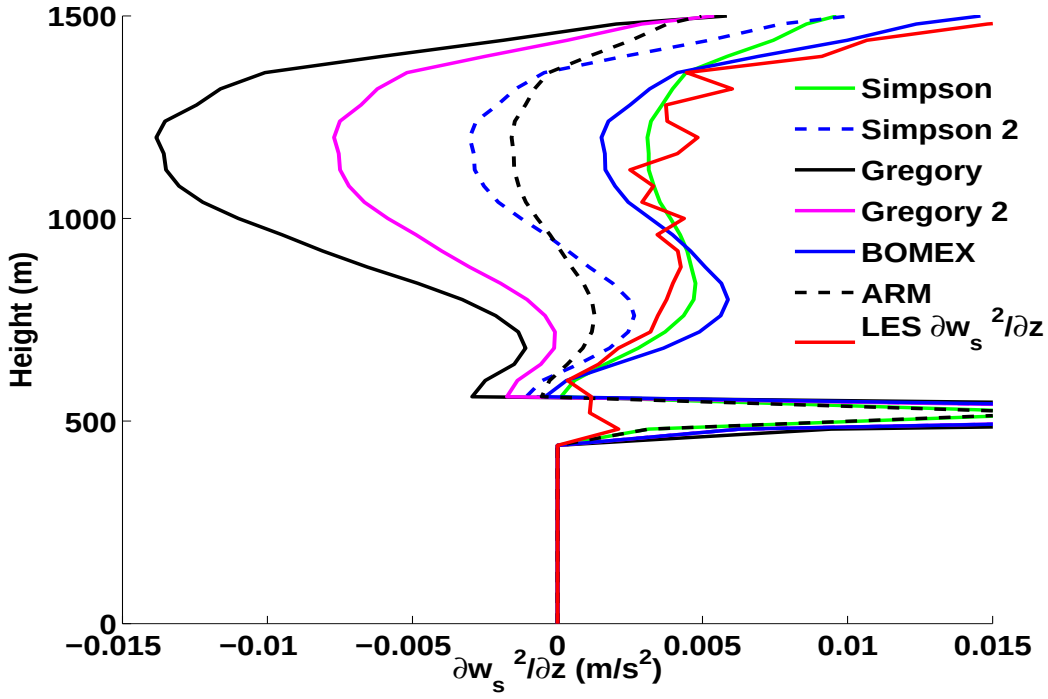

Figure 4.2: Comparison of the derivative of the vertical velocity squared calculated using the constants with the one calculated by the LES model for the 8$^{\text{th}}$ hour of simulation for the BOMEX case. The values for the constants belonging to the different authors can be found in table 4.1.

Figure 4.2 shows that the above proposed values for a and b give a much better result. However, the values suggested by Simpson and Wiggert (1969) ($a = 2/3$ and $b = 1$) give an even better solution.

Besides from the budgets the resolved vertical velocity squared is compared with the vertical velocity squared evaluated using the parameterization. The differential equation has been evaluated using the buoyancy and entrainment calculated by the LES model, as follows:

$$\begin{aligned} \psi &= w_s^2 \\ \psi[1] &= 0 \\ \frac{1}{2}\frac{\psi[n] - \psi[n-1]}{\delta z} &= aB[n] - b\varepsilon_{q_t}\psi[n] \end{aligned} \tag{4.1}$$

Here n denotes the height level which corresponds to a height of $40(n-1)$ meters since the model calculates the buoyancy and q_t values every 40 meters. We use this system to solve the vertical velocity squared for both the currently used and the suggested parameters derived from the LES results. The starting value is chosen to be zero because there is no cloud core present at the surface; cloud base is around 600 [m]. The results are displayed in figure 4.3.

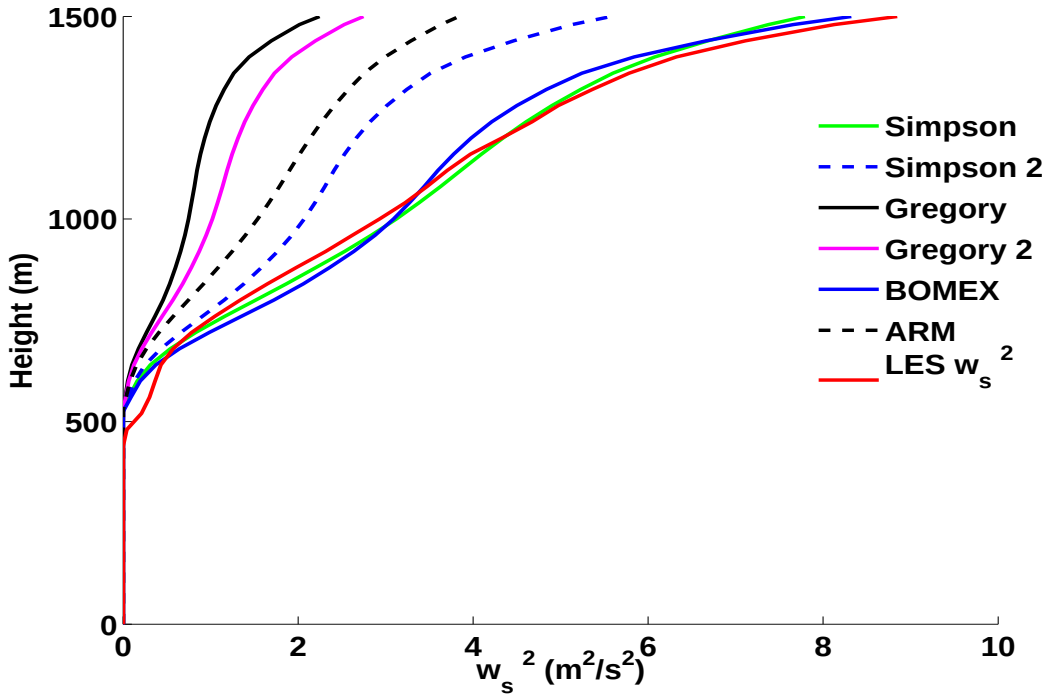

Figure 4.3: Comparison of the vertical velocity squared for the current and suggested parameter values for the 8$^{\text{th}}$ hour for the BOMEX case. The values for the constants belonging to the different authors can be found in table 4.1.

The vertical velocity squared is very close to the vertical velocity squared as calculated by the LES model for the suggested constants based on the LES data for the BOMEX case. Apparently $a = 1$ and $b = 2$ predicts almost the same vertical velocity as the constants $a = 2/3$ and $b = 1$. Both solutions are very close to the LES data. Both solutions would give the correct results for the vertical velocity squared, but based on the budgets (figure 4.2) taking the pressure effect into account through the prefactor a (scaling the buoyancy) is preferable. This is also what was found by Simpson and Wiggert (1969).

To further verify the findings and possibly find even better values an optimisation has been done with the data. We keep the constant $b = 1$, because both the BOMEX case and the ARM case, described in the next section, seem to support this theory. Here should be noted that table 4.1 gives another value based on the result of the LES BOMEX, but this is the result from observation of the budgets of the BOMEX case (figure 4.1). The comparisons of the gradient of the conditionally sampled vertical velocity squared (figure 4.2) and the conditionally sampled vertical velocity squared (figure 4.3) showed that keeping $b = 1$ gives an even better approximation.

For this optimisation the vertical velocity squared is calculated using the same procedure as above (4.1) (now referred to as w^2_{par}) for different values of a. The optimum value for the constant a is determined as the value for which the following is as small as possible:

$$\sum_{cloudbase}^{cloudtop} \left| w^2_{LES} - w^2_{par} \right| \tag{4.2}$$

Cloud base and cloud top are estimated based on the data, but do not need to be very precise. w_{LES} is the vertical velocity as calculated by the LES model.

This approach gives an optimum value for $a = 2/3$ like found by Simpson and Wiggert (1969) and also found above. There is hardly any difference between the various hours of simulation and this further supports the values found by Simpson and Wiggert (1969).

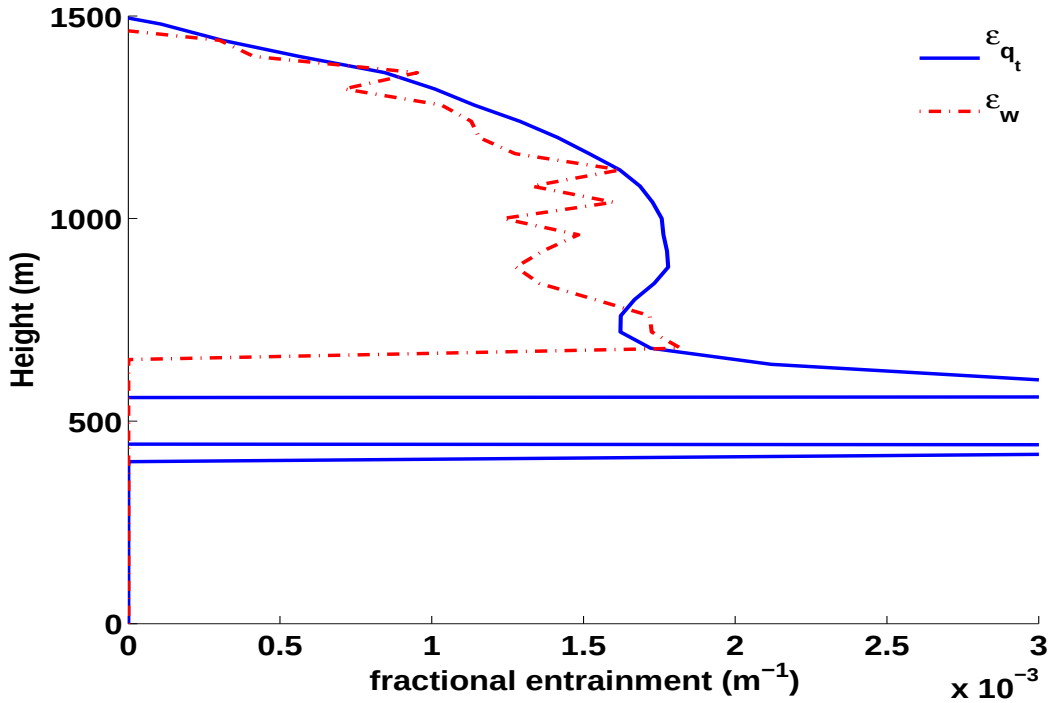

Figure 4.4: Fractional entrainment calculated using either the remainder of equation (3.21)(ε_w) or the q_t budget (3.23)(ε_{q_t}) for the 8$^{\text{th}}$ hour of simulation for the BOMEX case.

It should be noted that the fractional entrainment is calculated using q_t (3.23). When deriving the fractional entrainment directly from equation (3.21), thus calculating ε_w without the assumption that it is equal to ε_{q_t}. Using it to exactly close the equation we obtain a slightly different fractional entrainment and thus different results for the vertical velocity as calculated above. Figure 4.4 shows the fractional entrainment for the 8$^{\text{th}}$ hour using the two methods of calculation. The differences are relatively small, making the entrainment model with q_t (3.23) a good approximation. For the earlier hours the difference is either equal or smaller than shown for the 8$^{\text{th}}$ hour.

4.2 ARM case

For the ARM case the 7^{th} till the 12^{th} hour are used. Before the 7^{th} hour almost no clouds are observed, while after 12 hours of simulation the budgets will remain the same for a few hours, before changing again due to the diurnal cycle. This last period of the ARM case is not analysed and may yield other results then presented here. In the figures only the 9^{th} and 12^{th} hour are displayed. The 7^{th} and 8^{th} hour are roughly similar to the 9^{th} hour. The terms for the hours between the 9^{th} and the 12^{th} hour show a gradual change from their behaviour in the 9^{th} hour to that observed in the 12^{th} hour. The budgets are clearly different from those observed at the BOMEX case. From the budgets it is clear (figures 4.5 and 4.6) that the pressure term almost completely balances the buoyancy and is not similar to the entrainment term as found in the BOMEX case. Based on this case it would be more logical to scale the buoyancy to account for the pressure term, while again the subplume term seems sufficiently small to neglect it.

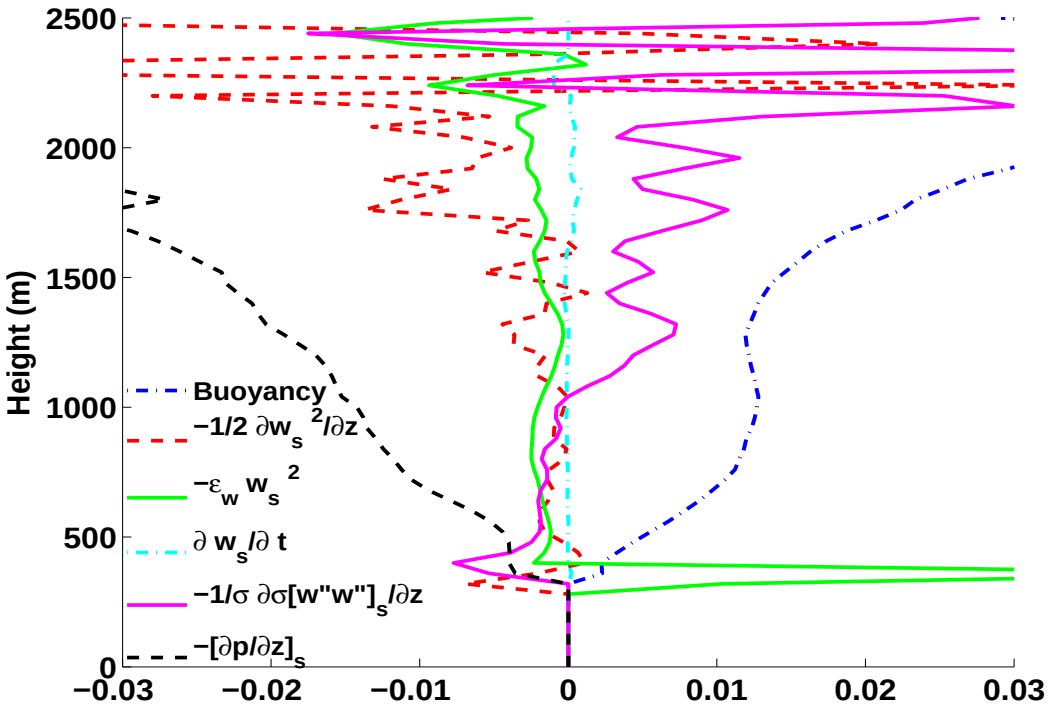

Figure 4.5: budgets of the vertical velocity equation (3.21) for the 9^{th} hour of simulation for the ARM case.

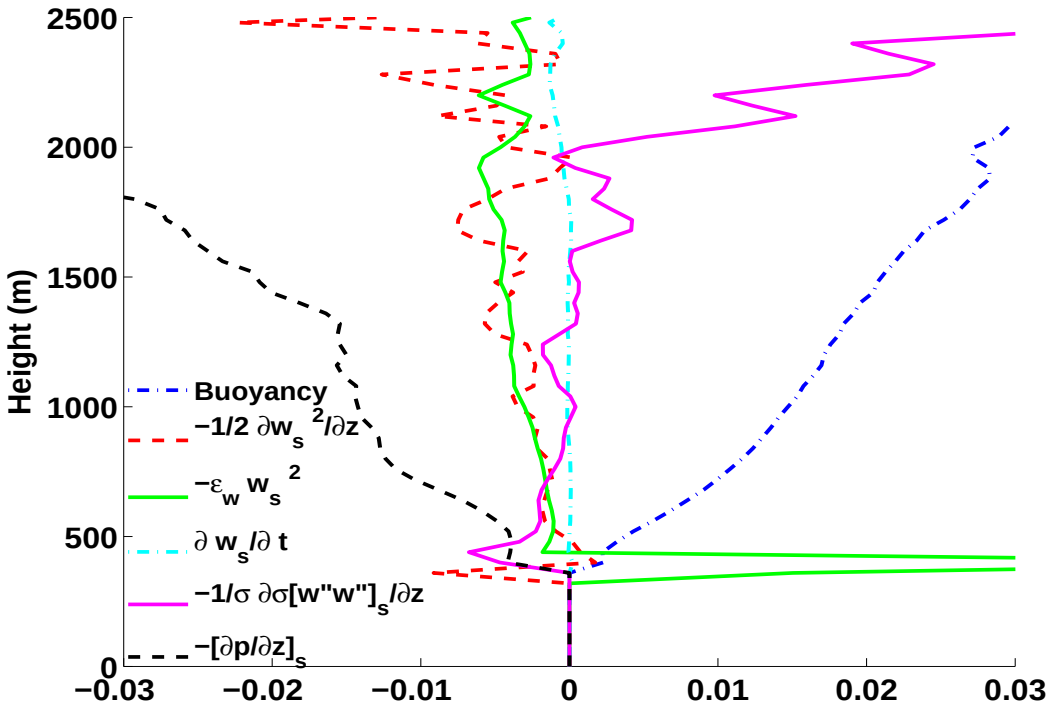

Figure 4.6: budgets of the vertical velocity equation (3.21) for the 12^{th} hour of simulation for the ARM case.

Using the same method as with the BOMEX case (4.1) to compare the vertical velocity, calculated with the various constants (table 4.1), with the result of the LES model. we see that the LES calculated value starts close to the parameterization with constants $a = {}^{1}/_{3}$ and $b = 2$ but later on approaches the parameterization with the constants $a = 2/3$ and $b = 2$ (figure 4.7). Between these values is the line for the constants $a = 1/3$ and $b = 1$. The last option seems most logical compared to the budget terms found. We also see a similarity for the relation between the constants as with the BOMEX case, the computed vertical velocity squared with the constants $a = 2/3$ and $b = 1$ and with the constants $a = 1$ and $b = 2$ are again almost equal.

The optimization done for the BOMEX case is also used for the ARM case and shows roughly the same. The optimum for the constant $a = 1/3$ is again found. Although for later hours it no longer holds. The optimum value for a then grows towards 1/2.

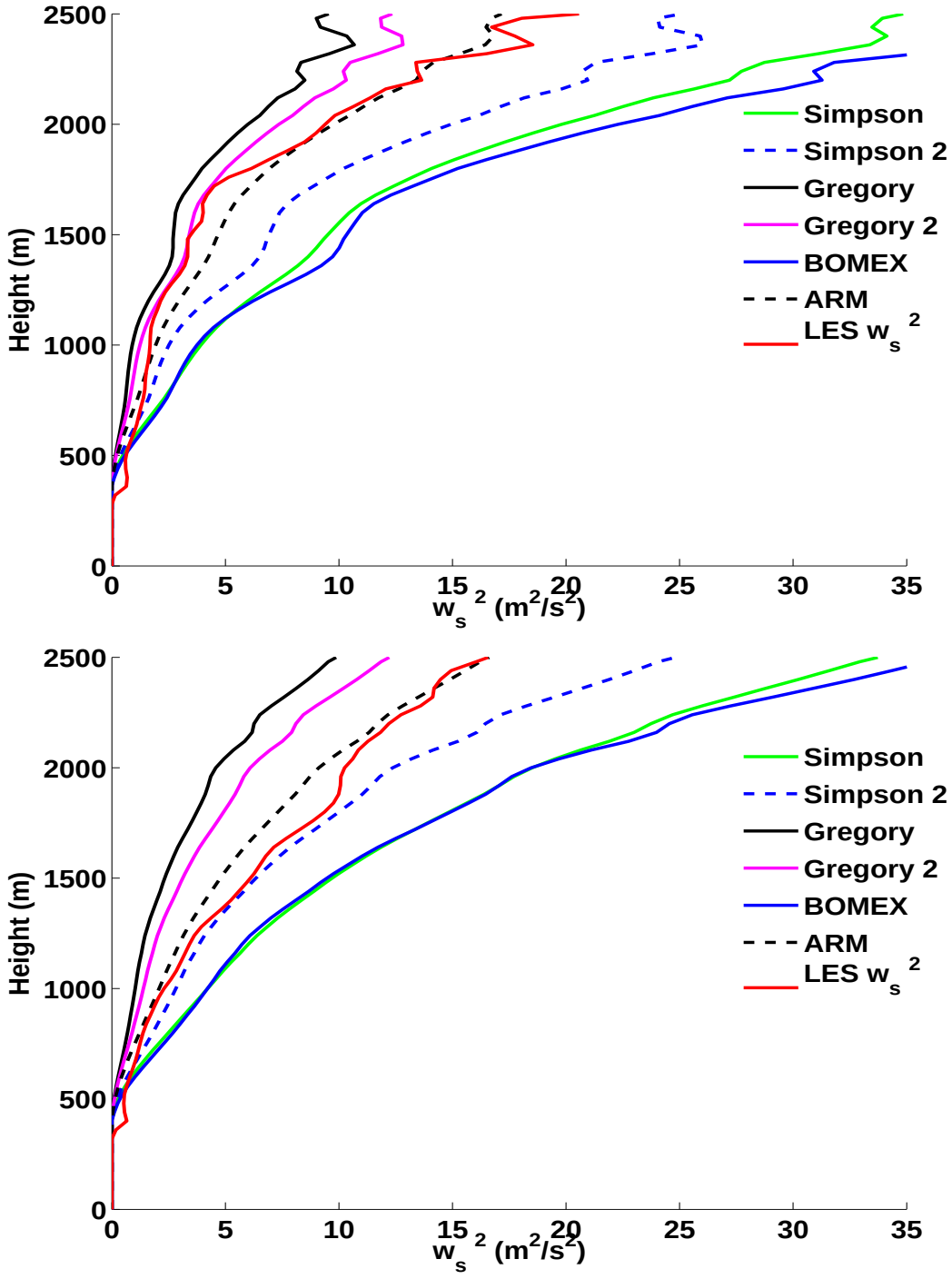

Figure 4.7: Comparison of the vertical velocity squared for the current and suggested parameter values for the 9^{th} (top) and the 12^{th} (bottom) hour for the ARM case. The values for the constants belonging to the different authors can be found in table 4.1.

A big difference is observed in the fractional entrainment. The fractional entrainment calculated through the q_t budget is roughly similar to that observed in the BOMEX case, however, it is completely different from the fractional entrainment calculated from the remainder of equation (3.21) (figures 4.8 and 4.9). The entrainment calculated from the remainder, thus the entrainment that would balance equation (3.21), is negative over the entire cloud.

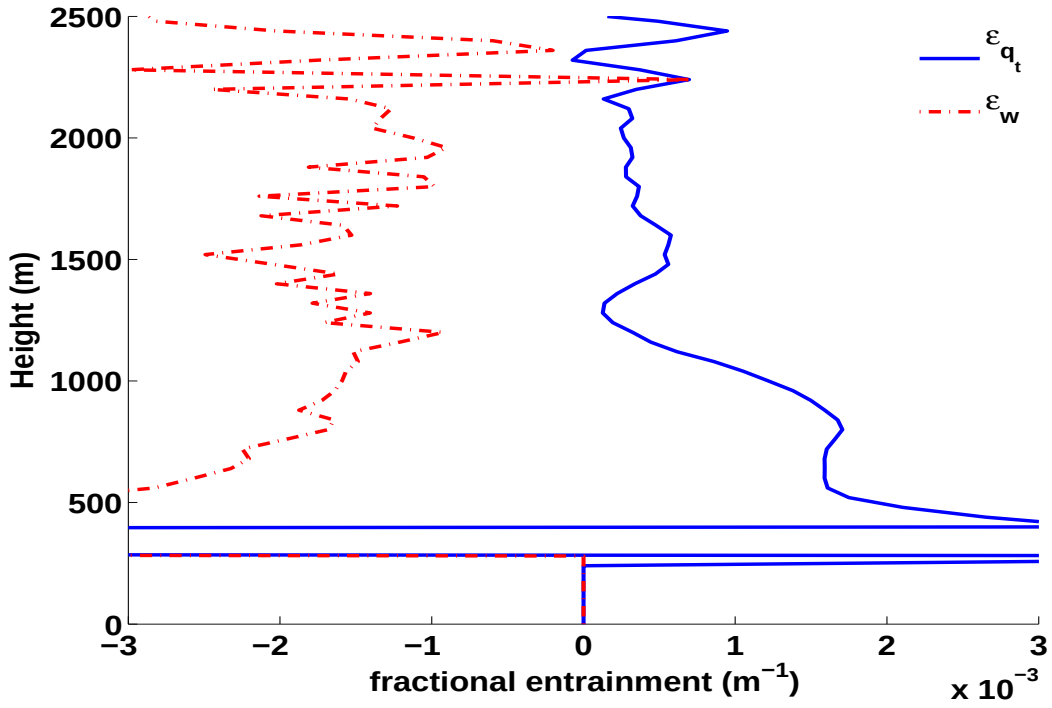

Figure 4.8: Fractional entrainment calculated using either the remainder of equation (3.21) or the q_t budget (3.23) for the 9$^{\text{th}}$ hour of simulation for the ARM case.

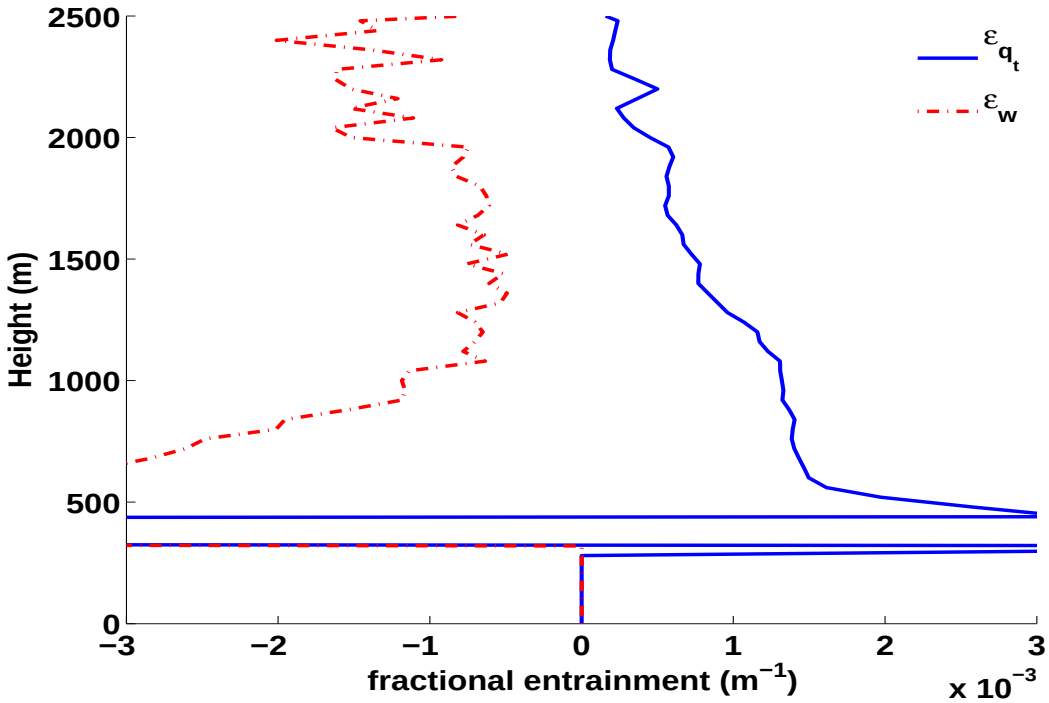

Figure 4.9: Fractional entrainment calculated using either the remainder of equation (3.21) or the q_t budget (3.23) for the 12$^{\text{th}}$ hour of simulation for the ARM case.

An explanation for the negative values of ε_w might be found in the subsiding shell. As shown by Heus (2008) the subsiding shell surrounding each cloud has a significant negative massflux compared to the upward massflux within the cloud. For smaller clouds the relative downward massflux of the shell, compared to the upward massflux in the cloud, is larger. The subsiding shell obviously influences the massflux and this effect scales with the cloud radius.

There can be two situations. In the first situation the area around the cloud core has a negative vertical velocity and thus moves downward. The area around the cloud core can also have a positive vertical velocity and thus move upward. Because the budget term in equation (3.14) contains the products $E_w w_e - D_w w_s$ and for this the assumption is made that the vertical velocity of the environment is negative, when the vertical velocity of the environment in the vicinity of the cloud is positive this could result in an negative fractional entrainment (ε_w). This could explain the difference between the two fractional entrainments (ε_w and ε_{q_t}). The two situations are sketched in figure (4.10).

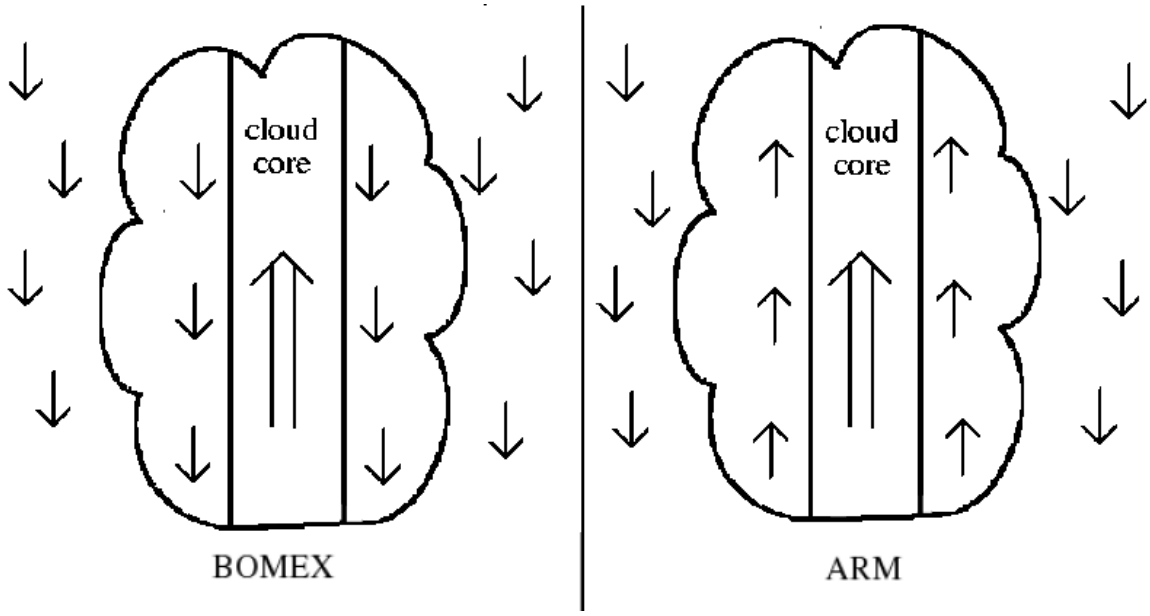

Figure 4.10: Illustration of the two possible situations with a subsiding shell around the cloud core. The arrows indicate the direction of the vertical velocity.

Heus (2008) showed that there is a clear subsiding shell around the clouds for the BOMEX case and within the shell the vertical velocity is negative. It can be argued that the shell surrounding the cloud core for the ARM case has a positive vertical velocity which gives rise to a negative fractional entrainment making the assumption $\varepsilon_w \approx \varepsilon_{q_t}$ false. This would have a obvious impact on the various terms of the parameterization and thus influence the constants.

5 Conclusion

A Comparison of all the conditionally sampled vertical velocity budgets from both cases shows that the leading force is the buoyancy, closely followed by both the lateral mixing and the pressure term. For the BOMEX case the pressure term is almost equal to the lateral mixing term, so the pressure term can easily be parameterized by scaling the lateral mixing with a factor of two. By resolving the vertical velocity squared from the parameterization and comparing it with the LES calculated vertical velocity squared, showed that scaling the lateral mixing term accurately predicts the vertical velocity. However, it is also possible to account for the pressure by scaling the buoyancy, which gives even better results, mainly when comparing the scaled budgets directly with the gradient of the vertical velocity squared, and is more in agreement with the ARM case.

The ARM case shows a different behaviour, here the pressure term is much larger than the lateral mixing term. The pressure term for the ARM case has the same (opposed) shape as the buoyancy term. Scaling the buoyancy to account for the pressure term gives an accurate prediction of the vertical velocity squared.

The constants with which the buoyancy is scaled for both cases is different. Because the pressure term in the ARM case is much larger compared to the buoyancy than in the BOMEX case, the scaling for the two cases is shown in figure 5.1.

Table 5.1: The best values for the constants a and b for the BOMEX and ARM cases for the parameterization (3.5).

Case	a	b
BOMEX	$2/3$	1
ARM	$1/3$	1

From these results it seems that the pressure term, that tends to damp the upward vertical velocity of a parcel of cloudy air, does this reduction with a factor of the buoyancy and together with the lateral mixing they are the main principles that describe the vertical velocity of a cloud parcel. Since the factor with which the pressure reduces the buoyancy is different for both cases, there is probably a dependency on some other parameter. The subplume term is so small that it can be neglected, rather then parameterized.

From the fractional entrainment calculated for both cases it seems that there is a major difference between the fractional entrainment calculated using a q_t budget and the entrainment needed to close the massflux based variant of the governing equations (3.21) for the ARM case, while there is almost no difference for the BOMEX case. An explanation for this can perhaps be found in the subsiding shell surrounding clouds. Heus (2008) showed that the subsiding shell can have a significant influence on the massflux. Within a subsiding shell it is possible that the vertical velocity is upward. In this case the fractional entrainment would be negative as is also seen in the LES data from the ARM case.

The research showed for both the ARM and BOMEX cases that it is possible to accurately describe the vertical velocity with the parameterization currently used, but the constants are different. Partly both from the currently used ones as from each other. Still scaling the buoyancy with a constant is possible although a measure or condition for the amount should be found.

A last note should be made to the fact that comparison of the vertical velocity squared resolved using the parameterization for different constants showed that choosing $a = 1$ and $b = 2$ results in the same vertical velocity squared as $a = {}^{2}/_{3}$ and $b = 1$. At this point there seems to be no reason why this should be the case, however both cases showed this same relation and perhaps there is a balance somewhere between these two constants that could be used in the future.

References

Brown, A. R., Cederwall, R. T., Chlond, A., Duynkerke, P. G., Golaz, J.-C., Khairoutdinov, M., Lewellen, D. C., Lock, A. P., Macvean, M. K., Moeng, C.-H., Neggers, R. A. J., Siebesma, A. P., and Stevens, B. (2002). Large-eddy simulation of the diurnal cycle of shallow umulus convection over land. *Quarterly Journal of the Royal Meteorological Society*, 128:1075–1093.

Cuijpers, J. W. M. (1994). *Large-Eddy Simulation of Cumulus Convection*. PhD thesis, Delft University of Technology.

de Roode, S. (2004). Clouds. Course Material.

de Roode, S. R. and Bretherton, C. S. (2003). Mass-flux budgets of shallow cumulus clouds. *Journal of the Atmospheric Sciences*, 60:137–151.

Deardoff, J. W. (1973). Three-dimensional numerical modeling of the planetary boundary layer. In Haugen, D. A., editor, *Workshop on Micrometeorology*, pages 271–311. American Meteorological Society.

Gregory, D. (2001). Estimation of entrainment rate in simple models of convective clouds. *Quarterly Journal of the Royal Meteorological Society*, 127:53–72.

Heus, T. (2008). *On the edge of a cloud*. PhD thesis, Delft University of Technology.

Holland, J. Z. and Rasmusson, E. M. (1973). Measurements of the atmospheric mass, energy, and momentum budgets over a 500–kilometer square of tropical ocean. *Monthly Weather Review*, 101(1):44–57.

Levine, J. (1959). Spherical vortex theory of bubble-like motion in cumulus clouds. *Journal of Meteorology*, 16:653–662.

Neggers, R. A. J., Duynkerke, P. G., and Rodts, S. M. A. (2003). Shallow cumulus convection: A validation of large-eddy simulation against aircraft and landsat observations. *Quarterly Journal of the Royal Meteorological Society*, 129:2671–2696.

Siebesma, A. P. (1998). *Buoyant Convection in Geophysical Flows*, chapter Shallow Cumulus Convection. Kluwer.

Siebesma, A. P., Bretherton, C. S., Brown, A., Chlond, A., Cuxart, J., Duynkerke, P. G., Jiang, H., Khairoutdinov, M., Lewellen, D., Moeng, C.-H., Sanchez, E., Stevens, B., and Stevens, D. E. (2003). A large eddy simulation intercomparison study of shallow cumulus convection. *Journal of the Atmospheric Siences*, 60(10):1201–1219.

Siebesma, A. P. and Cuijpers, J. W. M. (1995). Evaluation of parametric assumptions for shallow cumulus convection. *Journal of the Atmospheric Sciences*, 52(6):650–666.

Siebesma, A. P., Soares, P. M. M., and Teixeira, J. (2007). A combined eddy-diffusivity mass-flux approach for the convective boundary layer. *Journal of the Atmospheric Sciences*, 64:1230–1248.

Simpson, J., Simpson, R. H., Andrews, D. A., and Eaton, M. A. (1965). Experimental cumulus dynamics. *Reviews of Geophysics*, 3(3):387–431.

Simpson, J. and Wiggert, V. (1969). Models of precipitating cumulus towers. *Monthly Weather Review*, 97(7):471–489.

van Zanten, M. (2000). *Entrainment processes in stratocumulus*. PhD thesis, University of Utrecht.

Young, G. S. (1988). Turbulence structure of the convective boundary layer. part iii: The vertical velocity budgets of thermals and their environment. *Journal of the Atmospheric Sciences*, 45(14):2039–2049.